ACS APPLIED ENERGY MATERIALS

www.acsaem.org Article

# Multiblock Copolymer Anion-Exchange Membranes Derived from Vinyl Addition Polynorbornenes

Ryan Selhorst, Jamie Gaitor, Minjung Lee, Danielle Markovich, Yue Yu, Megan Treichel, Che Olavarria Gallegos, Tomasz Kowalewski, Lena F. Kourkoutis, Ryan C. Hayward, and Kevin J. T. Noonan*

Cite This: *ACS Appl. Energy Mater.* 2021, 4, 10273−10279 Read Online

ACCESS | Metrics & More | Article Recommendations | Supporting Information

**ABSTRACT:** Block copolymers have shown promise in ion-exchange membranes as they can phase separate into well-defined nanostructures which promote transport. Herein, a systematic study of multiblock copolymers containing cationic blocks is presented (diblock up to pentablock), and these were contrasted against a statistical copolymer. A series of vinyl addition polynorbornene anion-exchange membranes were prepared by copolymerization of 5-*n*-hexyl-2-norbornene and 5-(4-bromobutyl)-2-norbornene, followed by conversion of the halide to a trimethylammonium group. The hydroxide conductivities of all synthesized block copolymers were higher than the statistical copolymer, with the tetra and pentablock copolymers being the most conductive. The higher conductivity of the multiblocks is likely a combination of the increased surface-to-volume ratio (smaller domain sizes) improving the connectedness of ionic domains. Water uptake of the block copolymers was also dependent on the number and order of blocks. Copolymers with ionic blocks at one chain end took up more water than those where the ionic segments were confined to the chain interior. Finally, a method was developed to attach alkaline-stable tetraaminophosphonium cations to the bromo-functionalized statistical and pentablock polynorbornene. Interestingly, the synthesized phosphonium polymers had double the water uptake of their ammonium counterparts, which was attributed to the larger occupied volume of the phosphonium as compared to the ammonium group.

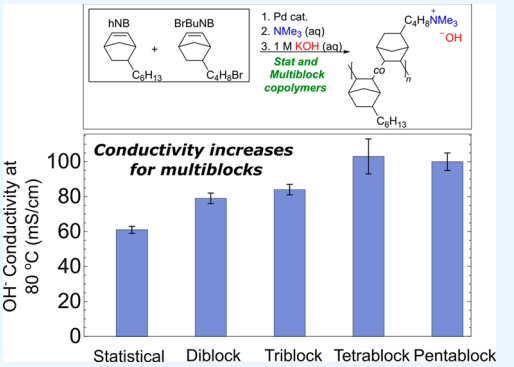


**KEYWORDS:** *multiblock copolymers, vinyl addition polynorbornenes, anion-exchange membranes, tetraaminophosphonium polymers, living polymerization*



## INTRODUCTION

Ion-exchange membranes are critical components in electrochemical cells, as they facilitate ion flux between the electrocatalysts.[1−5] In the last decade, there has been rising interest in membranes that promote the flow of hydroxide anions, as these materials can be used in alkaline fuel cells and electrolyzers.[1−5] Such anion-exchange membranes (AEMs) are typically comprised of polymers with covalently tethered cationic groups. Their mechanical integrity is governed by the polymer backbone, and anion movement is dictated by the cationic side chains.

Achieving high $OH^-$ conductivity ($\sigma$ > 80−100 mS/cm) in AEMs often requires relatively large concentrations of cationic groups appended to the polymer, especially compared to the number of charged groups in proton-exchange membranes (PEMs).[6] This difference may be due to the lower mobility of $OH^-$ in comparison with $H^+$ in aqueous environments.[7−10] Increasing the ion content in AEMs to improve performance can, however, be detrimental to swelling and mechanical integrity of the membrane.[6] This trade-off offers an opportunity to improve AEM materials through rational design.

Kohl and coworkers recently demonstrated that crosslink density can be used to largely control water uptake and conductivity in vinyl addition polynorbornene AEMs.[11−13] The authors prepared trimethylammonium-based statistical and block copolymers and found that light crosslinking produced materials with exceptional conductivity (190−200 mS/cm at 80 °C).[11−13] Moreover, the authors demonstrated that the linear tetrablock ammonium copolymer was stable in 1 M NaOH solution at 80 °C, with no loss in conductivity over 1200 h.[11]

**Received:** July 23, 2021
**Accepted:** August 10, 2021
**Published:** September 3, 2021

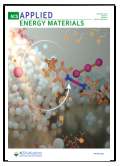




https://doi.org/10.1021/acsaem.1c02094
*ACS Appl. Energy Mater.* 2021, 4, 10273−10279

This study prompted us to consider the specific role of architecture in linear polynorbornenes and how this can be used to control properties. Herein, a statistical copolymer and a multiblock series were synthesized to explore the impact of polymer composition on hydroxide transport in AEM thin films. Block copolymers with pendant trimethylammonium cations produced higher conductivities than the statistical analogue. However, water uptake was higher for all of the block copolymers as compared to the statistical copolymer and moreover, it was impacted by the precise location of the ionic block (flanking or middle). Finally, a method was developed to tether base-stable tetraaminophosphonium cations to the statistical and pentablock polynorbornenes. While the statistical tetraaminophosphonium performed well as an AEM, excessive water uptake was observed with the pentablock, which likely arises from the combination of the phase separated ionic domains and the bulkier cation.

## RESULTS AND DISCUSSION

Block copolymers have been considered in AEMs to promote nanophase separation and transport,[14,15] with individual studies largely focused on a single polymer architecture (e.g., a di- or triblock).[16−24] Cationic multiblocks have also been prepared using step-growth polymerization previously,[25−29] but this approach does not easily enable precise control over the number of block segments in the final polymer. Sequential buildup of functional polymers was desired, to understand property differences when the functional unit is distributed statistically along the backbone versus in a block or multiblock architecture. Poly(5-*n*-alkylnorbornenes) were a natural choice for this study, as they have high glass transition temperatures[30] and can be solution-cast into mechanically stable, free-standing films.[31] Additionally, living vinyl addition polymerization of 5-*n*-alkylnorbornenes has been demonstrated previously with $^{t}Bu_3PPd(Me)Cl$ activated with salts of weakly coordinating anions such as sodium tetrakis[3,5-bis(trifluoromethyl)-phenyl]borate (BArF) (Figure 1A).[32−34] This catalyst system enabled preparation of high molecular weight copolymers from *endo*/*exo* mixtures of 5-*n*-hexyl-2-norbornene (hNB) and 5-(4-bromobutyl)-2-norbornene) (BrBuNB).

**Copolymer Synthesis.** Two different synthetic strategies were used to prepare the functional copolymer series (Figure 1A). A statistical copolymer was synthesized by direct combination of hNB and BrBuNB with the activated catalyst in $CH_2Cl_2$. Block copolymers were prepared by sequential addition of the hNB (A block) and BuBrNB (B block). Monomer consumption was monitored using $^1$H NMR spectroscopy in sequential addition experiments, to ensure complete conversion during each chain extension. Representative GPC traces are shown in Figure 1B, and final copolymers were isolated in all cases by precipitation into methanol.

A 2:1 ratio of hNB:BrBuNB was targeted for each copolymer to ensure a meaningful comparison across the series. This composition was also chosen to prevent excessive swelling in water upon conversion of the neutral polymer to the cationic trimethylammonium form (Figure 1A). $^1$H NMR spectra of the polymer samples confirmed that the percent incorporation of BrBuNB was typically within 5% of the target value (Figure S1 and Table S1). Moreover, good yields of the final materials were obtained in all cases (~75% or higher).

Targeted molecular weights for the copolymers were above the critical chain-entanglement for poly(5-*n*-hexylnorbornene),[35] with $M_n$ values for the series ranging between 80 and 130 kg/mol (determined relative to polystyrene standards). The individual block lengths decreased moving from the di- to pentablock, to maintain similar molecular weights across the series. A high molecular weight shoulder was observed in some chromatograms, along with tailing in the low molecular weight region, but this did not impact chain extension. The high molecular weight shoulder is apparent in the GPC traces for the diblock and pentablock copolymers in Figure 1B. Representative spectra and chromatograms are included in the Supporting Information (Figures S1−S9).

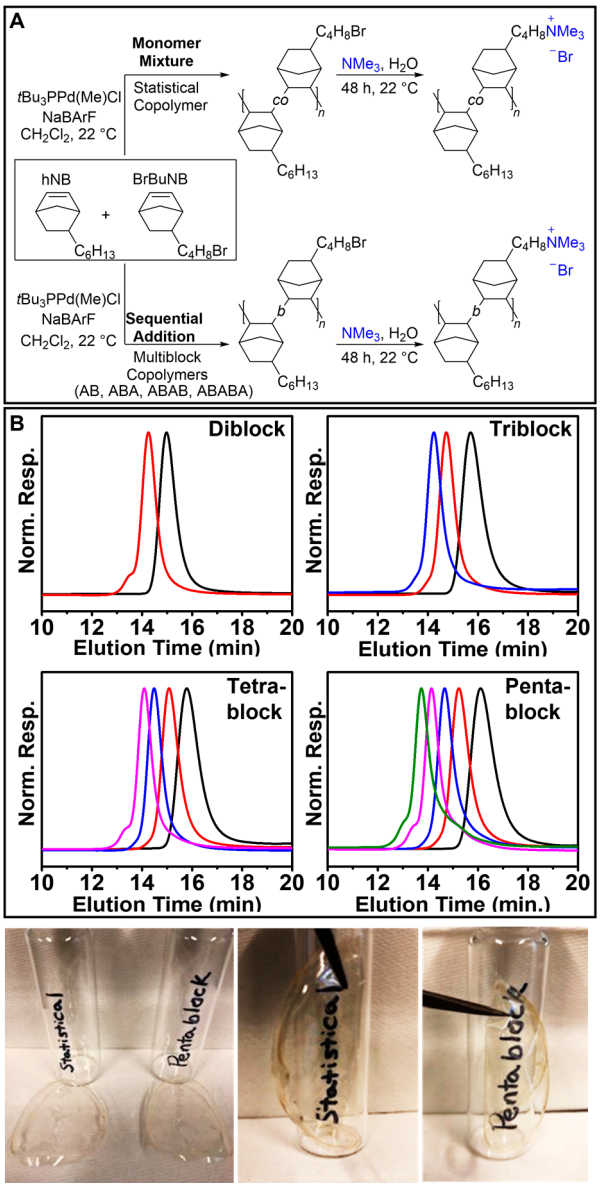


**Figure 1.** (A) Synthetic scheme of statistical (top) and multiblock copolymers (bottom) by vinyl addition polymerization. (B) Gel-permeation chromatography (GPC) traces of the multiblock copolymers. GPC traces were collected using THF as the eluent, and molecular weights were determined relative to polystyrene standards (refractive index detector). Diblock - $M_n$, 104 kg/mol; $Đ$, 1.16. Triblock - $M_n$, 100 kg/mol; $Đ$, 1.18. Tetrablock - $M_n$, 118 kg/mol; $Đ$, 1.18. Pentablock - $M_n$, 112 kg/mol; $Đ$, 1.38. (C) Photographs of the stat- and pentablock-$NMe_3$[Br] copolymer films.

Homogeneous free-standing films were obtained by dissolving the polymers in $CHCl_3$, followed by solvent evaporation in stainless steel Petri dishes. The films were


https://doi.org/10.1021/acsaem.1c02094
ACS Appl. Energy Mater. 2021, 4, 10273−10279

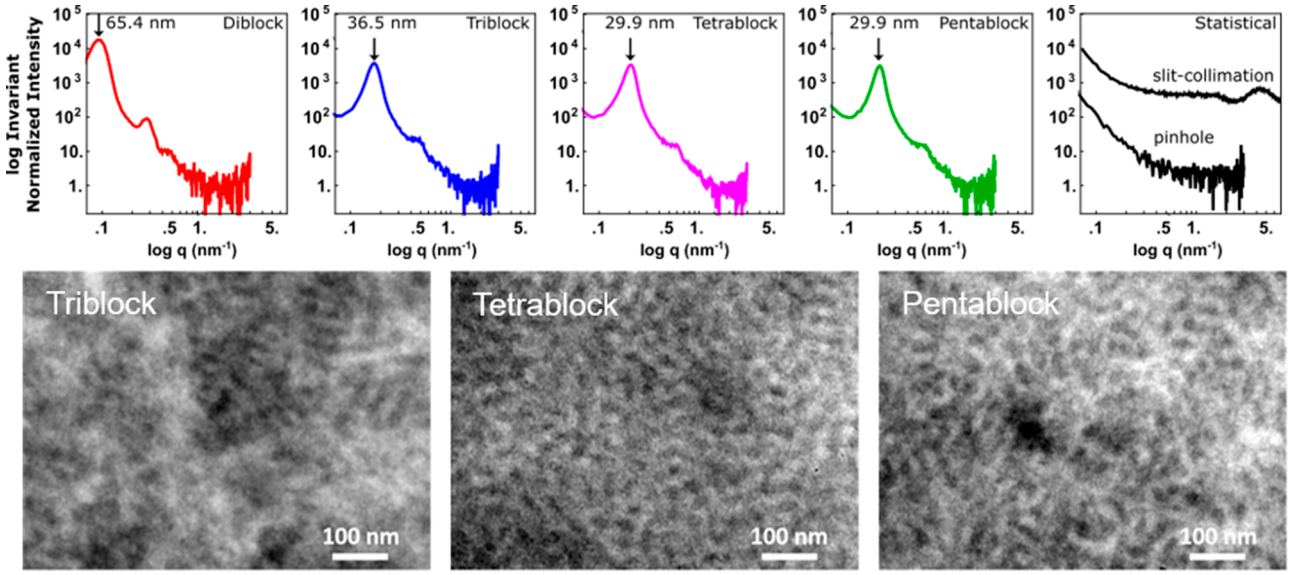


**Figure 2.** Top - SAXS scattering patterns acquired at 22 °C for a series of $NMe_3[Br]$ copolymer films in pinhole geometry (red - diblock with $M_n$, 104 kg/mol; $Đ$, 1.16; blue - triblock with $M_n$, 100 kg/mol; $Đ$, 1.18; magenta - tetrablock with $M_n$, 118 kg/mol; $Đ$, 1.18; green - pentablock with $M_n$, 112 kg/mol; $Đ$, 1.38; black - statistical with $M_n$, 125 kg/mol; $Đ$, 1.17). The SAXS pattern acquired in slit-collimation mode for the statistical copolymer is vertically shifted and included in the top right panel. Bottom - Cryo-TEM images of the triblock, tetrablock, and pentablock copolymers (left to right) taken at an accelerating voltage of 200 keV. Microphase separation is observed in all three copolymers with ordering length scales of 22−31 nm for the triblock, 32−40 nm for the tetrablock, and 28−34 nm for the pentablock as determined from fast Fourier transforms of the images.

removed from the dishes and then immersed in 28% (w/v) $NMe_{3(aq)}$ at room temperature for 48 h to afford the desired trimethylammonium polymers with a $Br^-$ counterion. Throughout the text, polymers are described by the copolymer type, cation, and counterion (e.g., stat-$NMe_3[Br]$). Photographs of the stat-$NMe_3[Br]$ and pentablock-$NMe_3[Br]$ copolymers are shown in Figure 1C.

$^1H$ NMR spectroscopy was used to confirm the loss of the $-CH_2-Br$ signal (3.4 ppm) and the appearance of the $N-CH_3$ signal at 3.00 ppm for the statistical copolymer. The di- and triblocks are only sparingly soluble in 1:1 $CDCl_3$:$CD_3OD$, and it was difficult to confirm full substitution using $^1H$ NMR spectroscopy. Fortunately, ion-exchange capacities (IECs) provided strong evidence that the substitution reaction with $NMe_3$ was effective, with values ranging from 1.6 to 1.7 mmol/g for all copolymers (Table S1), near the expected value of 1.72 mmol/g.

TGA analysis of these copolymers revealed onsets of decomposition ($T_d$ 5%) between 210 and 256 °C. These values fall below the expected glass transition temperature for the copolymers, so $T_g$'s were not determined (the $T_g$ of poly(5-*n*-hexylnorbornene) is 265 °C[30]). The decomposition temperature onsets for the stat-$NMe_3[Br]$ and diblock-$NMe_3[Br]$ (210 and 226 °C, respectively) are slightly lower than those of the tri-, tetra-, and pentablock-$NMe_3[Br]$ which all decompose near 255 °C (Figure S10). A two-step decomposition was observed for all copolymers. The first step corresponds to ∼10−15% loss, with nearly all of the remaining mass lost in the second step. Mass loss in the first step most likely arises from decomposition of the ionic group, followed by polymer decomposition in the second step.

**SAXS/TEM.** The nanostructure of the dried ammonium bromide copolymers was probed using small-angle X-ray scattering (SAXS) in the pinhole geometry (top of Figure 2) and narrow slit, large $q$ range collimation modes (Figure S11). In both instances, the scattering patterns for the block copolymers revealed the presence of a clear but broad primary Bragg peak at wavevector $q^*$, as well as a higher order peak at $3q^*$, indicating periodic nanoscale phase separation, although with limited long-range ordering. The $d$-spacing decreased with increasing number of blocks from ∼65 nm for the diblock to ∼30 nm for the tetra- and pentablock copolymers.

As expected, the Bragg peaks were absent in the statistical copolymer SAXS patterns (top right in Figure 2). Close inspection of the high $q$ range of the statistical copolymer traces acquired in slit collimation mode (top right in Figure 2) revealed the presence of a distinct change of slope in the ∼2 $nm^{-1}$ range. This feature was interpreted as the indication of the short-range, *aperiodic* clustering of ionic groups. Similar clustering has been observed in our recent study of phosphonium-based statistical copolymers.[36] In addition, patterns acquired in slit-collimated geometry (Figure S11) exhibited in all instances broad maxima centered at ∼5 $nm^{-1}$ corresponding to the wide angle scattering amorphous halos of all copolymers.

Real space morphologies of the triblock, tetrablock, and pentablock copolymers were visualized using cryogenic transmission electron microscopy (bottom of Figure 2). Electron transparent specimens, ∼70 nm in thickness, were prepared using cryo-microtomy to keep the membrane structure intact during the cutting and imaging processes. The inferior mechanical integrity of the diblock copolymer in comparison with multiblocks, which are stabilized by physical crosslinking, made it less amenable to sectioning. Dark regions in all of the images were identified as ionic block domains with electron density contrast arising from the presence of $Br^-$ counterions. Together with the SAXS data, these TEM images suggest a disordered cocontinuous structure or a lamellar morphology with only very short-range ordering. Length scales from TEM were also comparable to the spacings determined


https://doi.org/10.1021/acsaem.1c02094
ACS Appl. Energy Mater. 2021, 4, 10273−10279

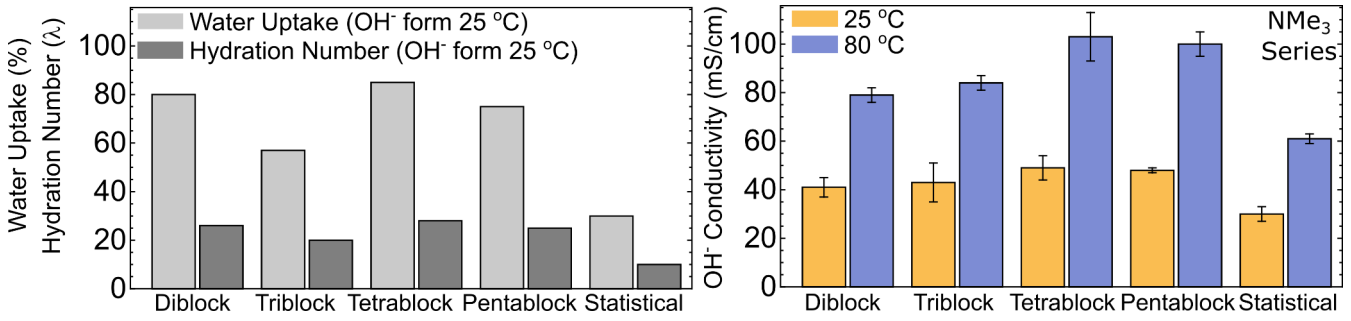


**Figure 3.** Left - Water uptake and hydration values for the statistical through pentablock-$NMe_3[OH]$. Water uptake was determined using gravimetric analysis. Hydration values were determined using the equation $\lambda = [1000 \times WU]/[IEC \times 18]$. Right - Conductivity ($\sigma$) for the statistical through pentablock-$NMe_3[OH]$ copolymer series determined using electrochemical impedance spectroscopy (EIS). The error is the standard deviation over three measurements. All other relevant parameters (e.g., $M_n$ values) for the copolymers are noted in Table S1.

from SAXS, although the images of the triblock suggested a less uniform morphology. This is evident from the presence of less defined regions within the image (left panel in the bottom of Figure 2).

**Water Uptake and Hydroxide Conductivity.** After the solid-state organization was evaluated, the $NMe_3[Br]$ copolymers were converted to the $^-OH$ form by immersion in 1 M KOH for 48 h at 60 °C. Water uptake, which was measured gravimetrically, ranged from 30 to 85% for the series (bar chart to the left in Figure 3). The stat-$NMe_3[OH]$ had the lowest water uptake at 30%, and the diblock- and tetrablock-$NMe_3[OH]$ had the highest, at 80 and 85%, respectively. The tri- and pentablock-$NMe_3[OH]$ had water uptakes in between these values at 57 and 75%, respectively. The slightly higher water uptakes of the diblock and tetrablock copolymers are likely a function of the ionic segments flanking one end of the polymer chain, leading to increased interchain ionic interactions. In contrast, the lower uptakes in the triblock and pentablock are likely attributed to the flanking location of the insulating blocks which enhances physical crosslinking and limits swelling. This is reminiscent of thermoplastic elastomers derived from ABA triblock copolymers where rigid outer A blocks flank the soft elastic B block. The water uptake for the tetrablock synthesized here (85%) was slightly higher in comparison to a previous report on ammonium-functionalized tetrablock polynorbornenes,[11] which might be due to the $M_n$ difference between the two samples (118 kg/mol compared to 38 kg/mol).

Hydroxide conductivity for the copolymer series was measured using electrochemical impedance spectroscopy (EIS) (specific details in the Supporting Information). Comparison across the series revealed an increase in conductivity for all block copolymers as compared to the statistical copolymer (bar chart to the right in Figure 3). An ~65% increase in conductivity is noted when comparing the statistical copolymer to the pentablock copolymer ($\sigma_{stat} = 60 \pm 2$ mS/cm versus $\sigma_{pent} = 100 \pm 5$ mS/cm at 80 °C). The conductivities of the tetra- and pentablock-$NMe_3[OH]$ copolymers are also ~25% higher than the di- and triblock-$NMe_3[OH]$ at 80 °C (Figure 3). Since the same concentration of ionic groups is being confined to smaller domains during microphase separation from diblock to pentablock, increasing the surface-to-volume ratio is likely affording more interconnected networks for ion transport. Nealey, Arges and coworkers have demonstrated that interconnected ionic domains enhance conductivity in lamellae-forming block copolymer electrolytes,[37,38] with minimization of defects and grain boundaries leading to large increases in ion conductivity. The multiblock architectures synthesized here likely improved the interconnectedness of ionic domains, which is consistent with the more uniform TEM images of the tetra- and pentablock, as compared to the triblock.

**Tetraaminophosphonium Polymers.** Considering the high hydroxide conductivity and controllable water uptake of the ammonium-functionalized polynorbornenes, we considered whether other cations could be appended to this polymer framework. Resonance-stabilized tetraaminophosphonium cations were targeted given their exceptional stability to alkaline media.[39,40] In past work, tetraaminophosphonium-based AEMs have been synthesized using ring-opening metathesis polymerization, with copolymerization of a cationic monomer and an insulating comonomer (e.g. norbornene or cyclooctene).[36,41] Here, the preparation of statistical and pentablock phosphonium copolymers was accomplished using post-polymerization modification (Figure 4).

A trisaminophosphazene $[N(iPr)Me]_3P{=}N{-}Me$ was combined with the hNB/BrBuNB copolymers in dichlorobenzene for nearly 2 days at 55 °C under $N_2$ (Figure 4). The trisaminophosphazene can be conveniently prepared from its protonated form using a two-phase reaction (Supporting Information). Both the statistical and pentablock copolymers were substituted successfully using this procedure, and workup followed by treatment with an anion-exchange resin produced the desired polymer in the $Cl^-$ form. New $^1H$ NMR signals arising from the phosphonium cation are noted in Figure 4.

The conversion of the pendant alkyl bromides to the phosphonium was estimated using $^1H$ NMR spectroscopy (Figure S3). The N−Me groups bound to the P atom appear between 2.5 and 2.8 ppm ($H_c$−$H_e$ in Figure 4). These were compared to the $CH_3$ group of the hNB which appears as a broad signal near 0.9 ppm. The integrals are within 10% of the expected value and suggest >90% conversion of the bromo group to the cationic tetraaminophosphonium (Figure S3). The stat- and pentablock-IPrMe[Cl] copolymers were solvent-cast from 1,2-dichloroethane/methanol to form flexible, free-standing films. After soaking the films in 1 M KOH for 48 h at 60 °C, water uptake, hydroxide conductivity, and IEC were measured. Bar charts comparing water uptake, hydration numbers, and hydroxide conductivity for the phosphonium and ammonium copolymers are shown in Figure 5.

First, the water uptake for the stat-IPrMe[OH] is approximately twice that of the stat-$NMe_3[OH]$ (59% versus 30%). The hydration number indicated that the phosphonium cation is solvated by nearly 3 times the number of $H_2O$


https://doi.org/10.1021/acsaem.1c02094
ACS Appl. Energy Mater. 2021, 4, 10273−10279

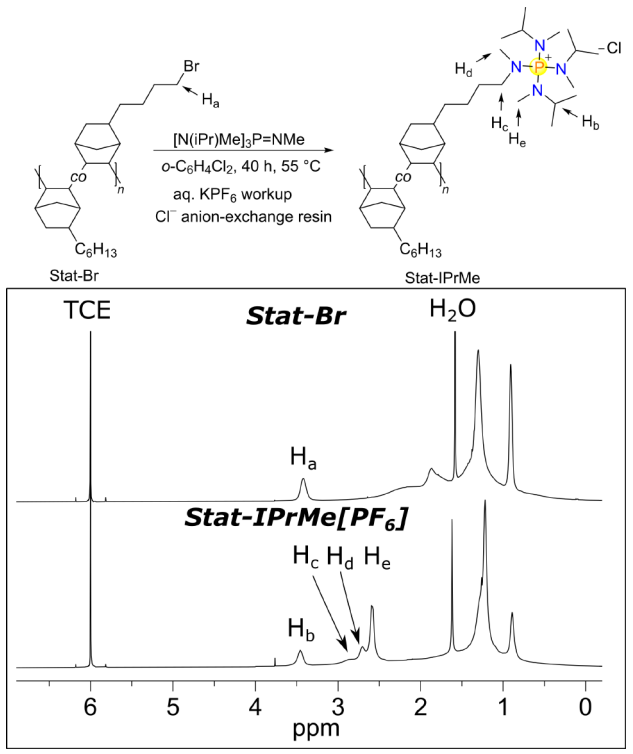


**Figure 4.** $^{1}$H NMR spectra before (top) and after (bottom) reaction of the statistical copolymer with the trisamino phosphazene [N(*i*Pr)Me]$_3$P═N—Me. Spectra were recorded in 1,1,2,2-tetrachloroethane-$d_2$ (TCE).

molecules when compared to the ammonium analogue (29 versus 10). This is consistent with the occupied volume for each cation. If the monomeric $NMe_4Cl$ (MW = 109.6 g/mol) and [(N(*i*Pr)Me)$_4$P]Cl (355.0 g/mol) salts are compared and assumed to have similar densities, at equimolar concentrations, the phosphonium cation will occupy ∼3.2 times the volume of the ammonium cation. Given this, it is not surprising that the hydration number for the stat-IPrMe[OH] is nearly 3 times larger than the stat-$NMe_3$[OH]. The water uptake is exacerbated in the pentablock copolymer, where the phosphonium variant is again double that of its ammonium counterpart (150% vs 75%). In both the ammonium and phosphonium copolymers, the change from a statistical to block copolymer resulted in higher water uptakes (Figure 5), but this is more problematic for the phosphonium copolymers where water uptakes are already higher.

The hydroxide conductivity of the stat-IPrMe[OH] at 25 and 80 °C was only slightly lower than the stat-$NMe_3$[OH] under identical conditions ($\sigma_{statIPrMe}$ = 52 ± 3 mS/cm vs $\sigma_{statNMe_3}$ = 61 ± 1 mS/cm at 80 °C). However, hydroxide conductivity for the phosphonium-functionalized pentablock was difficult to measure and unreliable at 80 °C due to excessive swelling. It was also only 15% better than the stat-IPrMe[OH] at room temperature. This is markedly different than in the ammonium copolymer series where an ∼65% increase in conductivity was noted from statistical to pentablock-$NMe_3$[OH]. This limitation of the pentablock-IPrMe[OH] is likely due to excessive water uptake, which limits its potential as an AEM. Blocks may prove difficult to work with for phosphonium-based systems, as the higher hydration of these bulky cations will likely result in water management issues, unless other strategies to mitigate water uptake are employed.

## CONCLUSIONS

In this study, a series of trimethylammonium-functionalized multiblock copolymers were synthesized by living vinyl addition polymerization. The impact of multiblock architecture on properties and transport was then systematically evaluated. The block copolymers were more conductive than the statistical variant, suggesting they should be of use as high performance hydroxide transporting membranes. The increase in conductivity was attributed to confining ammonium groups within a microphase separated block, which affords a better network for ion transport. The results are consistent with Kohl's prior work on tetrablock copolymers[11−13] and suggest that block copolymer phase segregation can be used as a tool to enhance conductivity. Interestingly, all of the block copolymers produced higher water uptakes than the statistical variant, suggesting that water management is more challenging with blocks. Moreover, in the block copolymers, the location of the ionic block (flanking or middle) had a small impact on water uptake, where middle blocks proved to be slightly more effective for controlling water uptake.

In addition, a method was developed to append resonance-stabilized tetraaminophosphonium cations to the statistical and pentablock copolymers. Direct comparison with the ammonium copolymers revealed much higher water uptake with

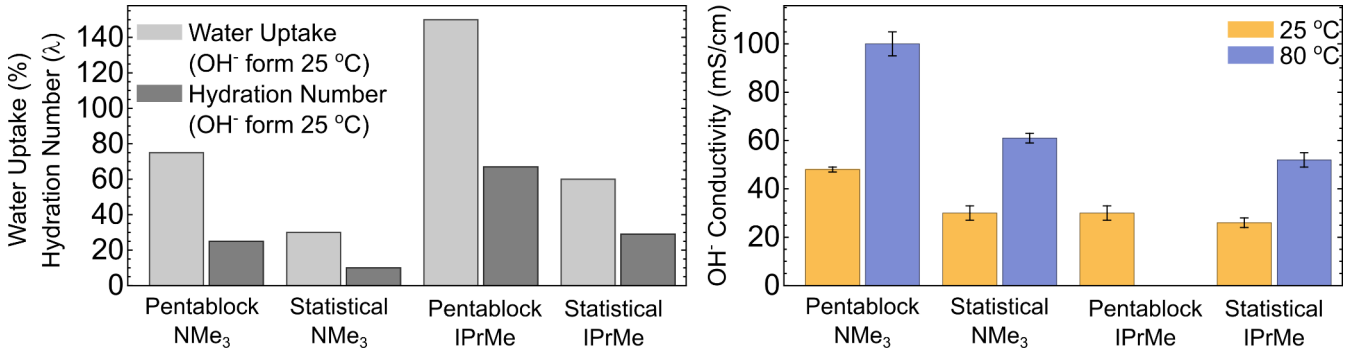


**Figure 5.** Left - Water uptake and hydration values for the statistical and pentablock $NMe_3$[OH] and IPrMe[OH] copolymers. Water uptake was determined using gravimetric analysis. Hydration values were determined using the equation $\lambda$ = [1000 × WU]/[IEC × 18]. Right - Conductivity ($\sigma$) for the trimethylammonium and tetraaminophosphonium copolymers determined in the $OH^-$ form using EIS. The error is the standard deviation over three measurements. Other relevant parameters (e.g., $M_n$ values) for the polymers are noted in Table S1.



https://doi.org/10.1021/acsaem.1c02094
ACS Appl. Energy Mater. 2021, 4, 10273−10279

these bulky cations appended to the polymer chain. Future work will look at other types of phosphonium cations and other classes of bulky cations to determine their impact on the performance and properties of polynorbornene membranes. We anticipate this study will provide useful guidance for future work aimed at polynorbornene membranes with cations beyond trimethylammonium.

## ■ ASSOCIATED CONTENT

### Supporting Information

The Supporting Information is available free of charge at https://pubs.acs.org/doi/10.1021/acsaem.1c02094.

Additional experimental details, materials and methods, protocols for polymer synthesis, NMR spectra, sample GPC traces, thermal property studies, small-angle X-ray scattering, and sample Nyquist plots (PDF)

## ■ AUTHOR INFORMATION


### Corresponding Author

**Kevin J. T. Noonan** − *Department of Chemistry, Carnegie Mellon University, Pittsburgh, Pennsylvania 15213, United States;* orcid.org/0000-0003-4061-7593; Email: noonan@andrew.cmu.edu

### Authors

**Ryan Selhorst** − *Department of Chemistry, Carnegie Mellon University, Pittsburgh, Pennsylvania 15213, United States*

**Jamie Gaitor** − *Department of Chemistry, Carnegie Mellon University, Pittsburgh, Pennsylvania 15213, United States*

**Minjung Lee** − *Department of Polymer Science & Engineering, University of Massachusetts Amherst, Amherst, Massachusetts 01003, United States*

**Danielle Markovich** − *School of Applied and Engineering Physics, Cornell University, Ithaca, New York 14853, United States*

**Yue Yu** − *School of Applied and Engineering Physics, Cornell University, Ithaca, New York 14853, United States*

**Megan Treichel** − *Department of Chemistry, Carnegie Mellon University, Pittsburgh, Pennsylvania 15213, United States*

**Che Olavarria Gallegos** − *Department of Chemistry, Carnegie Mellon University, Pittsburgh, Pennsylvania 15213, United States*

**Tomasz Kowalewski** − *Department of Chemistry, Carnegie Mellon University, Pittsburgh, Pennsylvania 15213, United States;* orcid.org/0000-0002-3544-554X

**Lena F. Kourkoutis** − *School of Applied and Engineering Physics and Kavli Institute at Cornell for Nanoscale Science, Cornell University, Ithaca, New York 14853, United States;* orcid.org/0000-0002-1303-1362

**Ryan C. Hayward** − *Department of Polymer Science & Engineering, University of Massachusetts Amherst, Amherst, Massachusetts 01003, United States; Department of Chemical and Biological Engineering, University of Colorado Boulder, Boulder, Colorado 80303, United States;* orcid.org/0000-0001-6483-2234

Complete contact information is available at: https://pubs.acs.org/10.1021/acsaem.1c02094


### Author Contributions

All authors have given approval to the final version of the manuscript.

### Notes

The authors declare no competing financial interest.

## ■ ACKNOWLEDGMENTS

The authors gratefully acknowledge financial support from the Center for Alkaline-Based Energy Solutions (CABES), an Energy Frontier Research Center funded by the U.S. Department of Energy, Office of Science, Basic Energy Sciences under Award No. DE-SC0019445. This work made use of the Cornell Center for Materials Research Shared Facilities which are supported through the NSF MRSEC program (DMR-1719875). Support for small-angle X-ray scattering characterization at UMass Amherst was provided by the U.S. Department of Energy, Office of Science, Basic Energy Sciences under Award No. DE-SC0016208. K.J.T.N. is grateful to Brian K. Long (University of Tennessee) for helpful discussions.

## ■ REFERENCES


(1) You, W.; Noonan, K. J. T.; Coates, G. W. Alkaline-Stable Anion Exchange Membranes: A Review of Synthetic Approaches. *Prog. Polym. Sci.* **2020**, *100*, 101177.

(2) Arges, C. G.; Zhang, L. Anion Exchange Membranes' Evolution toward High Hydroxide Ion Conductivity and Alkaline Resiliency. *ACS Appl. Energy Mater.* **2018**, *1*, 2991−3012.

(3) Hickner, M. A. Strategies for Developing New Anion Exchange Membranes and Electrode Ionomers. *Electrochem. Soc. Interface* **2017**, *26*, 69−73.

(4) Varcoe, J. R.; Atanassov, P.; Dekel, D. R.; Herring, A. M.; Hickner, M. A.; Kohl, P. A.; Kucernak, A. R.; Mustain, W. E.; Nijmeijer, K.; Scott, K.; Xu, T.; Zhuang, L. Anion-Exchange Membranes in Electrochemical Energy Systems. *Energy Environ. Sci.* **2014**, *7*, 3135−3191.

(5) Wang, Y.-J.; Qiao, J.; Baker, R.; Zhang, J. Alkaline Polymer Electrolyte Membranes for Fuel Cell Applications. *Chem. Soc. Rev.* **2013**, *42*, 5768−5787.

(6) Pan, J.; Chen, C.; Zhuang, L.; Lu, J. Designing Advanced Alkaline Polymer Electrolytes for Fuel Cell Applications. *Acc. Chem. Res.* **2012**, *45*, 473−481.

(7) Chen, M.; Zheng, L.; Santra, B.; Ko, H.-Y.; DiStasio, R. A.; Klein, M. L.; Car, R.; Wu, X. Hydroxide Diffuses Slower than Hydronium in Water Because its Solvated Structure Inhibits Correlated Proton Transfer. *Nat. Chem.* **2018**, *10*, 413−419.

(8) Agmon, N.; Bakker, H. J.; Campen, R. K.; Henchman, R. H.; Pohl, P.; Roke, S.; Thämer, M.; Hassanali, A. Protons and Hydroxide Ions in Aqueous Systems. *Chem. Rev.* **2016**, *116*, 7642−7672.

(9) Tuckerman, M. E.; Chandra, A.; Marx, D. Structure and Dynamics of $OH^-$(aq). *Acc. Chem. Res.* **2006**, *39*, 151−158.

(10) Tuckerman, M. E.; Marx, D.; Parrinello, M. The Nature and Transport Mechanism of Hydrated Hydroxide Ions in Aqueous Solution. *Nature* **2002**, *417*, 925−929.

(11) Mandal, M.; Huang, G.; Kohl, P. A. Anionic Multiblock Copolymer Membrane Based on Vinyl Addition Polymerization of Norbornenes: Applications in Anion-Exchange Membrane Fuel Cells. *J. Membr. Sci.* **2019**, *570-571*, 394−402.

(12) Mandal, M.; Huang, G.; Kohl, P. A. Highly Conductive Anion-Exchange Membranes Based on Cross-Linked Poly(norbornene): Vinyl Addition Polymerization. *ACS Appl. Energy Mater.* **2019**, *2*, 2447−2457.

(13) Mandal, M.; Huang, G.; Hassan, N. U.; Mustain, W. E.; Kohl, P. A. Poly(norbornene) Anion Conductive Membranes: Homopolymer, Block Copolymer and Random Copolymer Properties and Performance. *J. Mater. Chem. A* **2020**, *8*, 17568−17578.

(14) Elabd, Y. A.; Hickner, M. A. Block Copolymers for Fuel Cells. *Macromolecules* **2011**, *44*, 1−11.

(15) Li, N.; Guiver, M. D. Ion Transport by Nanochannels in Ion-Containing Aromatic Copolymers. *Macromolecules* **2014**, *47*, 2175−2198.
(16) Buggy, N. C.; Du, Y.; Kuo, M.-C.; Ahrens, K. A.; Wilkinson, J. S.; Seifert, S.; Coughlin, E. B.; Herring, A. M. A Polyethylene-Based Triblock Copolymer Anion Exchange Membrane with High Conductivity and Practical Mechanical Properties. *ACS Appl. Polym. Mater.* **2020**, *2*, 1294−1303.
(17) You, W.; Padgett, E.; MacMillan, S. N.; Muller, D. A.; Coates, G. W. Highly Conductive and Chemically Stable Alkaline Anion Exchange Membranes via ROMP of *trans*-Cyclooctene Derivatives. *Proc. Natl. Acad. Sci. U. S. A.* **2019**, *116*, 9729−9734.
(18) Zhang, W.; Liu, Y.; Jackson, A. C.; Savage, A. M.; Ertem, S. P.; Tsai, T.-H.; Seifert, S.; Beyer, F. L.; Liberatore, M. W.; Herring, A. M.; Coughlin, E. B. Achieving Continuous Anion Transport Domains Using Block Copolymers Containing Phosphonium Cations. *Macromolecules* **2016**, *49*, 4714−4722.
(19) Mohanty, A. D.; Ryu, C. Y.; Kim, Y. S.; Bae, C. Stable Elastomeric Anion Exchange Membranes Based on Quaternary Ammonium-Tethered Polystyrene-b-poly(ethylene-*co*-butylene)-b-polystyrene Triblock Copolymers. *Macromolecules* **2015**, *48*, 7085−7095.
(20) Li, Y.; Liu, Y.; Savage, A. M.; Beyer, F. L.; Seifert, S.; Herring, A. M.; Knauss, D. M. Polyethylene-Based Block Copolymers for Anion Exchange Membranes. *Macromolecules* **2015**, *48*, 6523−6533.
(21) Jeon, J. Y.; Tian, D.; Pagels, M. K.; Bae, C. Efficient Preparation of Styrene Block Copolymer Anion Exchange Membranes via One-Step Friedel−Crafts Bromoalkylation with Alkenes. *Org. Process Res. Dev.* **2019**, *23*, 1580−1586.
(22) Jeon, J. Y.; Park, S.; Han, J.; Maurya, S.; Mohanty, A. D.; Tian, D.; Saikia, N.; Hickner, M. A.; Ryu, C. Y.; Tuckerman, M. E.; Paddison, S. J.; Kim, Y. S.; Bae, C. Synthesis of Aromatic Anion Exchange Membranes by Friedel-Crafts Bromoalkylation and Cross-Linking of Polystyrene Block Copolymers. *Macromolecules* **2019**, *52*, 2139−2147.
(23) Lin, C. X.; Wu, H. Y.; Li, L.; Wang, X. Q.; Zhang, Q. G.; Zhu, A. M.; Liu, Q. L. Anion Conductive Triblock Copolymer Membranes with Flexible Multication Side Chain. *ACS Appl. Mater. Interfaces* **2018**, *10*, 18327−18337.
(24) Ertem, S. P.; Caire, B. R.; Tsai, T.-H.; Zeng, D.; Vandiver, M. A.; Kusoglu, A.; Seifert, S.; Hayward, R. C.; Weber, A. Z.; Herring, A. M.; Coughlin, E. B.; Liberatore, M. W. Ion Transport Properties of Mechanically Stable Symmetric ABCBA Pentablock Copolymers with Quaternary Ammonium Functionalized Midblock. *J. Polym. Sci., Part B: Polym. Phys.* **2017**, *55*, 612−622.
(25) Liu, L.; Ahlfield, J.; Tricker, A.; Chu, D.; Kohl, P. A. Anion Conducting Multiblock Copolymer Membranes with Partial Fluorination and Long Head-Group Tethers. *J. Mater. Chem. A* **2016**, *4*, 16233−16244.
(26) Weiber, E. A.; Meis, D.; Jannasch, P. Anion Conducting Multiblock Poly(arylene ether sulfone)s Containing Hydrophilic Segments Densely Functionalized with Quaternary Ammonium Groups. *Polym. Chem.* **2015**, *6*, 1986−1996.
(27) Park, D.-Y.; Kohl, P. A.; Beckham, H. W. Anion-Conductive Multiblock Aromatic Copolymer Membranes: Structure-Property Relationships. *J. Phys. Chem. C* **2013**, *117*, 15468−15477.
(28) Zhao, Z.; Wang, J.; Li, S.; Zhang, S. Synthesis of Multi-Block Poly(arylene ether sulfone) Copolymer Membrane with Pendant Quaternary Ammonium Groups for Alkaline Fuel Cell. *J. Power Sources* **2011**, *196*, 4445−4450.
(29) Tanaka, M.; Fukasawa, K.; Nishino, E.; Yamaguchi, S.; Yamada, K.; Tanaka, H.; Bae, B.; Miyatake, K.; Watanabe, M. Anion Conductive Block Poly(arylene ether)s: Synthesis, Properties, and Application in Alkaline Fuel Cells. *J. Am. Chem. Soc.* **2011**, *133*, 10646−10654.
(30) Grove, N. R.; Kohl, P. A.; Allen, S. A. B.; Jayaraman, S.; Shick, R. Functionalized Polynorbornene Dielectric Polymers: Adhesion and Mechanical Properties. *J. Polym. Sci., Part B: Polym. Phys.* **1999**, *37*, 3003−3010.
(31) Bermeshev, M. V.; Chapala, P. P. Addition Polymerization of Functionalized Norbornenes as a Powerful Tool for Assembling Molecular Moieties of New Polymers with Versatile Properties. *Prog. Polym. Sci.* **2018**, *84*, 1−46.
(32) Kim, D.-G.; Bell, A.; Register, R. A. Living Vinyl Addition Polymerization of Substituted Norbornenes by a t-$Bu_3$P-Ligated Methylpalladium Complex. *ACS Macro Lett.* **2015**, *4*, 327−330.
(33) Yamashita, M.; Takamiya, I.; Jin, K.; Nozaki, K. Syntheses and Structures of Bulky Monophosphine-Ligated Methylpalladium Complexes: Application to Homo- and Copolymerization of Norbornene and/or Methoxycarbonylnorbornene. *Organometallics* **2006**, *25*, 4588−4595.
(34) Lipian, J.; Mimna, R. A.; Fondran, J. C.; Yandulov, D.; Shick, R. A.; Goodall, B. L.; Rhodes, L. F.; Huffman, J. C. Addition Polymerization of Norbornene-Type Monomers. High Activity Cationic Allyl Palladium Catalysts. *Macromolecules* **2002**, *35*, 8969−8977.
(35) Müller, K.; Kreiling, S.; Dehnicke, K.; Allgaier, J.; Richter, D.; Fetters, L. J.; Jung, Y.; Yoon, D. Y.; Greiner, A. Synthesis and Rheological Properties of Poly(5-n-hexylnorbornene). *Macromol. Chem. Phys.* **2006**, *207*, 193−200.
(36) Treichel, M.; Womble, C. T.; Selhorst, R.; Gaitor, J.; Pathiranage, T. M. S. K.; Kowalewski, T.; Noonan, K. J. T. Exploring the Effects of Bulky Cations Tethered to Semicrystalline Polymers: The Case of Tetraaminophosphoniums with Ring-Opened Polynorbornenes. *Macromolecules* **2020**, *53*, 8509−8518.
(37) Kambe, Y.; Arges, C. G.; Czaplewski, D. A.; Dolejsi, M.; Krishnan, S.; Stoykovich, M. P.; de Pablo, J. J.; Nealey, P. F. Role of Defects in Ion Transport in Block Copolymer Electrolytes. *Nano Lett.* **2019**, *19*, 4684−4691.
(38) Arges, C. G.; Kambe, Y.; Dolejsi, M.; Wu, G.-P.; Segal-Pertz, T.; Ren, J.; Cao, C.; Craig, G. S. W.; Nealey, P. F. Interconnected Ionic Domains Enhance Conductivity in Microphase Separated Block Copolymer Electrolytes. *J. Mater. Chem. A* **2017**, *5*, 5619−5629.
(39) Womble, C. T.; Kang, J.; Hugar, K. M.; Coates, G. W.; Bernhard, S.; Noonan, K. J. T. Rapid Analysis of Tetrakis-(dialkylamino)phosphonium Stability in Alkaline Media. *Organometallics* **2017**, *36*, 4038−4046.
(40) You, W.; Hugar, K. M.; Selhorst, R. C.; Treichel, M.; Peltier, C. R.; Noonan, K. J. T.; Coates, G. W. Degradation of Organic Cations under Alkaline Conditions. *J. Org. Chem.* **2021**, *86*, 254−263.
(41) Noonan, K. J. T.; Hugar, K. M.; Kostalik, H. A., IV; Lobkovsky, E. B.; Abruña, H. D.; Coates, G. W. Phosphonium-Functionalized Polyethylene: A New Class of Base-Stable Alkaline Anion Exchange Membranes. *J. Am. Chem. Soc.* **2012**, *134*, 18161−18164.


https://doi.org/10.1021/acsaem.1c02094
*ACS Appl. Energy Mater.* 2021, 4, 10273−10279